Cadence and Position Tracking for Decoupled Legs during Switched Split-Crank Motorized FES-Cycling

F. I. Esquivel Estay*, C. A. Rouse*, M. H. Cohen*, C. A. Cousin*, W. E. Dixon*

***Abstract*—Functional electrical stimulation (FES) has proven to be an effective method for improving health and regaining muscle function for people with limited or reduced motor skills. Closed-loop control of motorized FES-cycling can facilitate recovery. Many people with movement disorders (e.g., stroke) have asymmetries in their motor control, motivating the need for a closed-loop control system that can be implemented on a split-crank cycle. In this paper, nonlinear sliding mode controllers are designed for the FES and electric motor on each side of a split-crank cycle to maintain a desired cadence and a crank angle offset of 180 degrees, simulating standard pedaling conditions. A Lyapunov-like function is used to prove stability and tracking of the desired cadence and position for the combined cycle-rider system. One experimental trial on an able-bodied individual demonstrated the feasibility and stability of the closed-loop controller, which resulted in an average cadence error of 2.62 ± 3.54 RPM for the dominant leg and an average position and cadence error of 39.84 ± 10.77 degrees and -0.04 ± 8.79 RPM for the non-dominant leg.**

I. Introduction

Functional electrical stimulation (FES) is the application of electrical impulses across muscle fibers to induce an involuntary muscle response or contraction. Over the last few decades, FES-induced cycling has become an established rehabilitation treatment for individuals with certain neurological disorders (NDs) since it has been shown to impart numerous physiological and psychological benefits.

Early literature in FES-cycling explored open-loop and linear proportional-derivative control of the stimulation intensity to achieve a functional task [1]–[3]; however, neither open-loop nor linear control addresses the nonlinearities of the uncertain cycle-rider system. In addition, a more coordinated cycling motion can be obtained by switching control input between stimulation of the quadriceps femoris, gluteal, and hamstring muscle groups and an electric motor at different points throughout the crank cycle [4]; however, the introduction of a switched system requires additional analysis since switching between stable subsystems can create instabilities in the overall system [5], [6]. Thus, more recent FES-cycling literature has focused on Lyapunov-based nonlinear control methods for switched systems with the goal of tracking cadence [4], [7]–[10] and power output [11], [12].

Most FES-cycling studies have been carried out using cycles with a traditional single crank design where the pedals are mechanically fixed at 180 degrees of separation. Although these studies have shown a high degree of relevance in rehabilitation treatments [13]–[18], the coupled dynamics of single-crank designs fail to isolate individual contributions of each leg. Numerous NDs, such as a stroke or localized muscle atrophy, can cause neuromuscular asymmetries in which a patient may exhibit a higher degree of strength on one side of their body than the other. Thus, individuals with asymmetries may significantly depend on one limb to reach the desired cycling goal, neglecting contributions of the less responsive limb [19]. Efforts to symmetrically involve both limbs during cycling have used torque measurements on a single crank cycle [20]. Additionally, decoupled bike pedals as in [21], [22] enable each limb to perform independently of the other; however, neither FES nor nonlinear control was implemented on the aforementioned studies.

Although motivation exists to further explore the benefits of decoupled cranks in FES-cycling studies, implementing closed-loop controllers for such systems presents additional considerations. A cadence goal is a common tracking objective in FES-cycling, but even if both legs are initialized at positions with 180 degrees of separation and are tasked with tracking the same cadence goal, over time, error accumulation may cause the legs to become out of phase. Thus, for this work, one leg will be denoted as the dominant system and the other will be referred to as the non-dominant system. The objective of the dominant side is to track a desired cadence, whereas the non-dominant side is tasked with tracking the cadence of, and 180 degree position offset from, the dominant leg, to maintain a natural cycling motion.

In this paper, a split-crank cycle is introduced and controllers for the motors and FES are developed for the switched control system. Separate switching signals for each side are implemented where the control signal switches between muscle groups and the electric motor as a function of crank angle. Motivated to address physiological asymmetries, two independent dynamic subsystems are analyzed, corresponding to each leg. Each subsystem is examined independently with a Lyapunov-like switched system stability analysis and the overall autonomous, two-leg, state-dependent, switched control system achieves global exponential stability,

*Department of Mechanical and Aerospace Engineering, University of Florida, Gainesville FL 32611-6250, USA Email: {fidelesquivel, courtneyarouse, maxhcohen, ccousin, wdixon}@ufl.edu

This research is supported in part by NSF award numbers DGE-1842473 and 1762829. Any opinions, findings and conclusions, or recommendations expressed in this material are those of the author(s) and do not necessarily reflect the views of the sponsoring agency.

provided sufficient gain conditions are met. Experimental results from an able-bodied participant are presented to characterize the performance of the subsequently designed controllers.

II. Model

The switched cycle-rider dynamics are modeled as[1]

$$\tau_{e_l}(t) \triangleq \tau_{c_l}(\dot{q}_l, \ddot{q}_l, t) + \tau_{r_l}(q_l, \dot{q}_l, \ddot{q}_l, t), \quad (1)$$

$\forall l \in L$ where the subscript $l \in L = \{dom, non\}$ indicates the dominant and non-dominant legs, respectively; $q_l : \mathbb{R}_{>0} \to \mathcal{Q}$ denotes the measurable crank angle for each side; and $\mathcal{Q} \subseteq \mathbb{R}$ denotes the set of all possible crank angles. The torques applied about the crank axis by the electric motor, the cycle, and the rider are denoted by $\tau_{e_l} : \mathbb{R}_{\geq 0} \to \mathbb{R}$, $\tau_{c_l} : \mathbb{R}^2 \times \mathbb{R}_{\geq 0} \to \mathbb{R}$, and $\tau_{r_l} : \mathcal{Q} \times \mathbb{R}^2 \times \mathbb{R}_{\geq 0} \to \mathbb{R}$, respectively. The torque applied about the crank axis by the cycle can be expressed as

$$\tau_{c_l}(\dot{q}_l, \ddot{q}_l, t) \triangleq J_{c_l}(q_l)\ddot{q}_l + b_c\dot{q}_l + d_{c_l}(t), \quad (2)$$

$\forall l \in L$, where $J_{c_l} : \mathcal{Q} \to \mathbb{R}_{>0}$, $b_{c_l} \in \mathbb{R}_{>0}$, and $d_{c_l} : \mathbb{R}_{\geq 0} \to \mathbb{R}$ denote inertial effects, viscous damping effects, and disturbances applied by the cycle, respectively. The torque applied about the crank by the rider can be separated into passive torques, $\tau_{p_l} : \mathcal{Q} \times \mathbb{R}^2 \to \mathbb{R}$, the FES induced muscle contribution, $\tau_{M_l} : \mathcal{Q} \times \mathbb{R} \times \mathbb{R}_{\geq 0} \to \mathbb{R}$, and the disturbances in the load, $d_{r_l} : \mathbb{R}_{\geq 0} \to \mathbb{R}$ as follows:

$$\begin{aligned} \tau_{r_l}(q_l, \dot{q}_l, \ddot{q}_l, t) \triangleq\ & \tau_{p_l}(q_l, \dot{q}_l, \ddot{q}_l) \\ & -\tau_{M_l}(q_l, \dot{q}_l, t) + d_{r_l}(t), \end{aligned} \quad (3)$$

$\forall l \in L$. It is assumed that the rider does not contribute volitionally to this experiment, and all volitional contributions are therefore included into the disturbance term $d_{r_l} : \mathbb{R}_{\geq 0} \to \mathbb{R}$. In (3), the passive torques applied by the rider are

$$\begin{aligned} \tau_{p_l}(q_l, \dot{q}_l, \ddot{q}_l) =\ & M_{p_l}(q_l)\ddot{q}_l(t) + V_l(q_l, \dot{q}_l)\dot{q}_l \\ & +G_l(q_l) + P_l(q_l, \dot{q}_l), \end{aligned} \quad (4)$$

where $M_{p_l} : \mathcal{Q} \to \mathbb{R}_{>0}$, $V_l : \mathcal{Q} \times \mathbb{R} \to \mathbb{R}$, $G_l : \mathcal{Q} \to \mathbb{R}$, and $P_l : \mathcal{Q} \times \mathbb{R} \to \mathbb{R}$ denote the inertial, centripetal-Coriolis, gravitational, and passive viscoelastic tissue forces of the rider's legs, respectively. With no volitional contribution, the torques applied by the muscles are denoted as the sum of each muscle's individual contribution by FES as

$$\tau_{M_l}(q_l, \dot{q}_l, t) \triangleq \sum_{m \in \mathcal{M}} B_{m_l}(q_l, \dot{q}_l)\, u_{m_l}(q_l, t), \quad (5)$$

$\forall m \in \mathcal{M}, \forall l \in L$, where the subscript $m \in \mathcal{M} = \{Q, G, H\}$ indicates the quadriceps femoris (Q), gluteal (G), and hamstring (H) muscle groups, respectively, and $u_{m_l} : \mathcal{Q} \times \mathbb{R} \times \mathbb{R}_{\geq 0} \to \mathbb{R}$ is the designed muscle control current input. The uncertain muscle control effectiveness is denoted by $B_{m_l} : \mathcal{Q} \times \mathbb{R} \to \mathbb{R}_{>0}$, $\forall m \in \mathcal{M}$ as in [4], [23]. The portion of each crank cycle in which a particular muscle group is stimulated is denoted by $\mathcal{Q}_{m_l} \subset \mathcal{Q}$. In this manner, $\mathcal{Q}_{m_l}$ is defined for each muscle group as

$$\mathcal{Q}_{m_l} \triangleq \{q_l \in \mathcal{Q} \mid T_{m_l}(q_l) > \varepsilon_{m_l}\}, \quad (6)$$

$\forall m \in \mathcal{M}, \forall l \in L$, where the function $T_{m_l} : \mathcal{Q} \to \mathbb{R}$ denotes the torque transfer ratio between each muscle group and the crank [23] and $\varepsilon_{m_l} \in \left(0,\ \max\left(T_{m_l}\right)\right]$ is the lower threshold for each torque transfer ratio, such that each muscle group is engaged only when it contributes positive crank motion. Based on (6), the piece-wise switching signal $\sigma_{m_l}(q_l) \in \{0, 1\}$ is defined for each muscle group such that $\sigma_{m_l}(q_l) = 1$ when $q_l \in \mathcal{Q}_{m_l}$ and $\sigma_{m_l}(q_l) = 0$ when $q_l \notin \mathcal{Q}_{m_l}$, $\forall m \in \mathcal{M}$, $\forall l \in L$. The region of the crank cycle where FES produces efficient torques, $\mathcal{Q}_{FES_l}$, is defined as $\mathcal{Q}_{FES_l} \triangleq \underset{m \in \mathcal{M}}{\cup}\{\mathcal{Q}_{m_l}\}, \forall m \in \mathcal{M}, \forall l \in L$ as defined in [8].

The electrical stimulation intensity applied to each muscle is defined as

$$u_{m_l} \triangleq \sigma_{m_l}(q)\, k_{m_l} u_{s_l}(t), \quad (7)$$

$\forall m \in \mathcal{M}, \forall l \in L$, where the subsequently designed FES control input is denoted by $u_{s_l}(t)$ and $k_{m_l} \in \mathbb{R}_{>0}$ is a constant control gain, $\forall m \in \mathcal{M}, \forall l \in L$.

Also from (1), the torque applied about the crank axis by the electric motor for each side can be expressed as

$$\tau_{e_l}(t) \triangleq B_{e_l} u_{e_l}(t), \quad (8)$$

$\forall m \in \mathcal{M}, \forall l \in L$, where $B_{e_l} \in \mathbb{R}_{>0}$ relates the electric motor's input current to the resulting torque about the crank axis, and $u_{e_l} : \mathbb{R}_{>0} \to \mathbb{R}$ is the designed electric motor controller. Substituting (2)-(5), 7, and 8 into (1) yields[2]

$$\begin{aligned} B_{M_l} u_{s_l} + B_{e_l} u_{e_l} =\ & M_l\ddot{q}_l + b_{c_l}\dot{q}_l + d_{cl} \\ & +V_l\dot{q}_l + G_l + P_l + d_{r_l}, \end{aligned} \quad (9)$$

$\forall l \in L$, where $B_{M_l} : \mathcal{Q} \times \mathbb{R} \to \mathbb{R}$ is the combined switched FES control effectiveness, defined as $B_{M_l} \triangleq \sum_{m \in \mathcal{M}} B_{m_l}\sigma_{m_l}k_{m_l}, \forall m \in \mathcal{M}, \forall l \in L$, and $M_l : \mathcal{Q} \to \mathbb{R}$ is defined as the summation $M_l \triangleq J_{c_l} + M_{p_l}$.

The subsequent development is based on the assumption that a dominant lower limb is identified and the non-dominant subsystem depends on the dominant subsystem, but the reverse is not applicable. Both subsystems are autonomous and state-dependent.

The switched system in (9) has the following properties and assumptions, $\forall l \in L$, as listed in [24].

Property: 1 $c_m \leq M_l \leq c_M$, where $c_m, c_M \in \mathbb{R}_{>0}$ are known constants. **Property: 2** $|V_l| \leq c_V|\dot{q}_l|$, where $c_V \in \mathbb{R}_{>0}$ is a known constant. **Property: 3** $|G_l| \leq c_G$, where $c_G \in \mathbb{R}_{>0}$ is a known constant. **Property: 4** $|P_l| \leq c_{P1} + c_{P2}|\dot{q}_l|$, where $c_{P1}, c_{P2} \in \mathbb{R}_{>0}$ are known constants. **Property: 5** $b_{c_l}\dot{q}_l \leq c_b|\dot{q}_l|$, where $c_b \in \mathbb{R}_{>0}$ is a known constant. **Property: 6** $|d_{r_l} + d_{c_l}| \leq c_d$, where $c_d \in \mathbb{R}_{>0}$ is a known constant. **Property: 7** $\frac{1}{2}\dot{M}_l = V_l$. **Property: 8** B_{m_l} has a lower bound $\forall m_l$, and thus, when

[1] For notational brevity, all explicit dependence on time, t, within the terms $q(t)$, $\dot{q}(t)$, $\ddot{q}(t)$ is suppressed.

[2] For notational brevity, all functional dependencies are hereafter suppressed unless required for clarity of exposition.

$\sum_{m\in\mathcal{M}} \sigma_{m_l} > 0$, $c_{b_M} \leq B_{M_l}$, where $c_{b_M} \in \mathbb{R}_{>0}$. **Property: 9** $c_{b_e} \leq B_e \leq c_{B_e}$, where c_{b_e}, $c_{B_e} \in \mathbb{R}_{>0}$.

III. Control Development

The two sides of the cycle-rider system are considered as dominant and non-dominant subsystems. The following control development is applicable to any combination of position and/or cadence objectives for each subsystem. Without loss of generality, in this paper the control objective is for the dominant subsystem to track a desired cadence and the non-dominant subsystem to track position and cadence such that a constant phase shift of 180 degrees from the dominant leg is maintained. Switching signals for the FES muscle control and the electric motor control for both legs are denoted as $\sigma_{s_l} : \mathbb{R}_{\geq 0} \to \{0, 1\}$ and $\sigma_{e_l} : \mathbb{R}_{\geq 0} \to \{0, 1\}$, respectively, $\forall l \in L$, $\forall m \in \mathcal{M}$. These signals are designed as

$$\sigma_{s_l} \triangleq \begin{cases} 1 & \text{if } q_l \in \mathcal{Q}_{m_l} \\ 0 & \text{if } q_l \notin \mathcal{Q}_{m_l} \end{cases}, \tag{10}$$

$$\sigma_{e_l} \triangleq \begin{cases} 1 & \text{if } q_l \notin \mathcal{Q}_{m_l} \\ 0 & \text{if } q_l \in \mathcal{Q}_{m_l} \end{cases}. \tag{11}$$

A. Dominant Subsystem

The control objective for the dominant subsystem is to track a desired cadence which is quantified by the cadence error $e_1 : \mathbb{R}_{\geq 0} \to \mathbb{R}$, defined as

$$e_1 \triangleq \dot{q}_{dom_d} - \dot{q}_{dom}, \tag{12}$$

where $\dot{q}_{dom_d}$, $\dot{q}_{dom} \in \mathbb{R}_{>0}$ are the desired and measured cadences for the dominant leg. Taking the time derivative of (12), multiplying by M_{dom}, and substituting into (9) yields

$$M_{dom}\dot{e}_1 = \chi_{dom} - V_{dom}e_1 - B_{e_{dom}}u_{e_{dom}} - B_{M_{dom}}u_{s_{dom}}, \tag{13}$$

where the auxiliary term $\chi_{dom} : Q \times \mathbb{R} \times \mathbb{R}_{\geq 0} \to 0$ is defined as $\chi_{dom} \triangleq b_{c_{dom}}\dot{q}_{dom} + d_{c_{dom}} + G_{dom} + P_{dom} + d_{r_{dom}} + V_{dom}\dot{q}_{dom_d} + M_{dom}\ddot{q}_{dom_d}$. Using Properties 1-6, χ_{dom} can be bounded as

$$\chi_{dom} \leq c_1 + c_2|e_1|, \tag{14}$$

where c_1, $c_2 \in \mathbb{R}_{>0}$ are constants, and $|\cdot|$ denotes the absolute value. Based on (12)-(14), and the subsequent stability analysis in Section IV, the muscle control input for the FES acting in the dominant subsystem is defined as

$$u_{s_{dom}} = \sigma_{s_{dom}}(k_1 e_1 + k_2 sgn(e_1)), \tag{15}$$

where $k_1, k_2 \in \mathbb{R}_{>0}$ are selectable constant control gains, and $\sigma_{s_{dom}}$ is defined in (10). Likewise, the switched controller for the dominant subsystem's electric motor is defined as

$$u_{e_{dom}} = \sigma_{e_{dom}}(k_3 e_1 + k_4 sgn(e_1)), \tag{16}$$

where k_3, $k_4 \in \mathbb{R}_{>0}$ are constant control gains, and $\sigma_{e_{dom}}$ is defined in (11). Substituting (15) and (16) into (13) results in the closed-loop error system for the dominant subsystem

$$\begin{aligned} M_{dom}\dot{e}_1 \;=\; & -B_{M_{dom}}\sigma_{s_{dom}}(k_1 e_1 + k_2 sgn(e_1)) \\ & -B_{e_{dom}}\sigma_{e_{dom}}(k_3 e_1 + k_4 sgn(e_1)) \\ & +\chi_{dom} - V_{dom}e_1. \end{aligned} \tag{17}$$

B. Non-dominant Subsystem

The control objective of the non-dominant subsystem is to track the desired crank angle, which is offset by 180 degrees from the dominant leg's position, and cadence. This objective is quantified by the position error $e_2 : \mathbb{R}_{\geq 0} \to \mathbb{R}$ and the auxiliary error $r : \mathbb{R}_{\geq 0} \to \mathbb{R}$, defined as

$$e_2 \triangleq q_{non_d} - q_{non}, \tag{18}$$

$$r \triangleq \dot{e}_2 + \alpha e_2, \tag{19}$$

where $q_{non} \in \mathbb{R}$ and $\alpha \in \mathbb{R}_{>0}$, are the measured crank angle for the non-dominant leg and a selectable control gain, respectively. The desired crank angle for the non-dominant leg is denoted by $q_{non_d} \in \mathbb{R}$ and defined as $q_{non_d} \triangleq q_{dom} - \pi$. The switching signal for the FES muscle control and the electric motor control for the non-dominant leg are defined in (10) and (11), respectively, where $l = non$ and $m \in \mathcal{M}$. Taking the time derivative of (19), multiplying by M_{non}, and substituting into (9) yields

$$M_{non}\dot{r} = \chi_{non} - V_{non}r - B_{e_{non}}u_{e_{non}} - B_{M_{non}}u_{s_{non}} - e_2, \tag{20}$$

where the auxiliary term $\chi_{non} : Q \times \mathbb{R} \times \mathbb{R}_{\geq 0} \to 0$ is defined as $\chi_{non} \triangleq M_{non}(\ddot{q}_{non_d} + \alpha\dot{e}_2) + b_{c_{non}}\dot{q}_{non} + d_{c_{non}} + P_{non} + d_{r_{non}} + V_{non}(\dot{q}_{non_d} + \alpha e_2) + G_{non} + e_2$. Based on (19), and Properties 1-6, χ_{non} can be bounded as

$$\chi_{non} \leq c_3 + c_4\|z\| + c_5\|z\|^2, \tag{21}$$

where c_3, c_4, $c_5 \in \mathbb{R}_{>0}$ are known constants, and the error vector $z \in \mathbb{R}^2$ is defined as $z = [e_2\ r]^T$. Based on (19)-(21), and the subsequent stability analysis in Section IV, the muscle control input acting on the non-dominant subsystem is defined as

$$u_{s_{non}} = \sigma_{s_{non}}\left(k_5 r + sgn(r)\left[k_6 + k_7\|z\| + k_8\|z\|^2\right]\right), \tag{22}$$

where k_5, k_6, k_7, $k_8 \in \mathbb{R}_{>0}$ are selectable control gains, and $\sigma_{s_{non}}$ was defined in (10). Likewise, the switched controller for the electric motor is defined as

$$u_{e_{non}} = \sigma_{e_{non}}\left(k_9 r + sgn(r)\left[k_{10} + k_{11}\|z\| + k_{12}\|z\|^2\right]\right), \tag{23}$$

where k_9, k_{10}, k_{11}, $k_{12} \in \mathbb{R}_{>0}$ are selectable constant control gains, and $\sigma_{e_{non}}$ was defined in (11). Substituting (22) and (23) into (20) results in the closed-loop error system for the non-dominant subsystem

$$\begin{aligned} M\dot{r} \;=\; & -B_{M_{non}}\sigma_{s_{non}}(k_5 r + sgn(r)[k_6 + k_7\|z\| \\ & +k_8\|z\|^2]) - B_{e_{non}}\sigma_{e_{non}}(k_9 r + sgn(r)[k_{10} \\ & +k_{11}\|z\| + k_{12}\|z\|^2]) + \chi_{non} - V_{non}r - e_2. \end{aligned} \tag{24}$$

IV. Stability Analysis

The stability analysis is divided into dominant and non-dominant subsystems. Four theorems are presented to evaluate the stability of the motor and FES controllers developed in Section III. To facilitate the analysis of a combination of position-based and velocity-based switching, switching times are denoted by $\left\{t^i_{n,l}\right\}$, $i \in \{s, e\}$, $n \in \{0, 1, 2, ...\}$, $\forall l \in$

L, where each $t^i_{n,l}$ represents the nth time that the system switches to activate stimulation (denoted by $i = s$) or the electric motor (denoted by $i = e$).

A. Dominant Subsystem

Let $V_{L_1} : \mathbb{R} \to \mathbb{R}_{\geq 0}$ be a positive definite, continuously differentiable, common Lyapunov function candidate defined as

$$V_{L_1} = \frac{1}{2} M_{dom} e_1^2, \tag{25}$$

which is radially unbounded and satisfies the following inequalities

$$(\frac{c_m}{2}) e_1^2 \leq V_{L_1} \leq (\frac{c_M}{2}) e_1^2, \tag{26}$$

where c_m and c_M are defined in Property 1. Taking the time derivative of (25) and using (17) and Property 7,

$$\begin{aligned} \dot{V}_{L_1} = \quad & e_1 \left(\chi_{dom} - B_{M_{dom}} \sigma_{s_{dom}} \left(k_1 e_1 + k_2 sgn\left(e_1\right) \right) \right. \\ & \left. - B_{e_{dom}} \sigma_{e_{dom}} \left(k_3 e_1 + k_4 sgn\left(e_1\right) \right) \right). \end{aligned} \tag{27}$$

Theorem 1. *For $q_{dom} \in \mathcal{Q}_{FES_{dom}}$, the cadence error system defined in (12) is exponentially stable, provided some gain conditions are satisfied.*

Proof: When $q_{dom} \in \mathcal{Q}_{FES_{dom}}$, $\sigma_{s_{dom}} = 1$ and $\sigma_{e_{dom}} = 0$. Therefore, the expression in (27) can be written as

$$\dot{V}_{L_1} = e_1 \left(\chi_{dom} - B_{M_{dom}} \left(k_1 e_1 + k_2 sgn\left(e_1\right) \right) \right). \tag{28}$$

Using (14), the following upper bound on (28) can be developed

$$\dot{V}_{L_1} \leq - \left(k_2 c_{b_M} - c_1 \right) |e_1| - \left(k_1 c_{b_M} - c_2 \right) e_1^2, \tag{29}$$

where c_{b_M} was defined in Property 8, k_1 was introduced in (15), and c_2 was introduced in (14). Equation (29) is negative definite, provided some gain conditions are satisfied, and can be algebraically manipulated to yield exponential convergence $\forall t \in \left[t^s_{n,\, dom},\, t^e_{n+1,\, dom} \right)$, $\forall n \in \{0, 1, 2...\}$. ■

Theorem 2. *For $q_{dom} \notin \mathcal{Q}_{FES_{dom}}$, the cadence error system defined in (12) is exponentially stable, provided some gain conditions are satisfied.*

Proof: When $q_{dom} \notin \mathcal{Q}_{FES_{dom}}$, $\sigma_{s_{dom}} = 0$ and $\sigma_{e_{dom}} = 1$. Therefore, the expression in (27) can be expressed as

$$\dot{V}_{L_1} = e_1 (\chi_{dom} - B_{e_{dom}} (k_3 e_1 + k_4 sgn(e_1))). \tag{30}$$

Upper bounding (30) using (14) and Property 9, yields

$$\dot{V}_{L_1} \leq -(k_4 c_{b_e} - c_1)|e_1| - (k_3 c_{b_e} - c_2) e_1^2, \tag{31}$$

which is negative definite provided gain conditions are satisfied, and can be solved to yield exponential convergence $\forall t \in \left[t^e_{n,\, dom},\, t^s_{n+1,\, dom} \right)$, $\forall n \in \{0, 1, 2...\}$. ■

Remark 1. By Theorems 1 and 2, and since V_{L1} is a common Lyapunov function for switching between FES and the motor on the dominant side, exponential convergence of the dominant subsystem is guaranted $\forall q_{dom} \in Q$.

B. Non-dominant Subsystem

Let $V_{L_2} : \mathbb{R} \to \mathbb{R}_{\geq 0}$ be a positive definite, continuously differentiable, common Lyaponov function candidate defined as

$$V_{L_2} = \frac{1}{2} M_{non} r^2 + \frac{1}{2} e_2^2, \tag{32}$$

and is radially unbounded and satisfies the following inequalities

$$\lambda_i ||z||^2 \leq V_{L_2} \leq \lambda_j ||z||^2, \tag{33}$$

where $\lambda_i, \lambda_j \in \mathbb{R}_{>0}$ are known constants. Using (24) and Property 7, the time derivative of (32) can be expressed as

$$\begin{aligned} \dot{V}_{L_2} \quad = \quad & r\chi_{non} - rB_{M_{non}} \sigma_{s_{non}} (k_5 r + sgn(r)[k_6 \\ & + k_7 \|z\| + k_8 \|z\|^2]) - rB_{e_{non}} \sigma_{e_{non}} (k_9 r \\ & + sgn(r)[k_{10} + k_{11} \|z\| + k_{12} \|z\|^2]) - \alpha e_2^2. \end{aligned} \tag{34}$$

Theorem 3. *For $q_{non} \notin \mathcal{Q}_{FES_{non}}$, the error system defined in (18) and (19) is exponentially stable, provided some gain conditions are satisfied.*

Proof: When $q_{non} \notin \mathcal{Q}_{FES_{non}}$, $\sigma_{s_{non}} = 0$ and $\sigma_{e_{non}} = 1$. Therefore, the expression in (34) can be reduced to

$$\begin{aligned} \dot{V}_{L_2} \quad = \quad & r\chi_{non} - \alpha e_2^2 - rB_{e_{non}} \left(k_9 r \right. \\ & \left. + sgn\left(r\right) \left[k_{10} + k_{11} ||z|| + k_{12} ||z||^2 \right] \right). \end{aligned} \tag{35}$$

Upper bounding (35) using (21) and Property 9, yields

$$\begin{aligned} \dot{V}_{L_2} \quad \leq \quad & -c_{b_e} k_9 r^2 - \alpha e_2^2 - \left(c_{b_e} k_{10} - c_3 \right) |r| \\ & - \left(c_{b_e} k_{11} - c_4 \right) |r| \ \|z\| - \left(c_{b_e} k_{12} - c_5 \right) |r| \ \|z\|^2, \end{aligned} \tag{36}$$

which is negative definite, provided gain conditions are satisfied, and can be solved to yield exponential convergence $\forall t \in \left[t^e_{n.\, non}, t^s_{n+1,\, non} \right)$, $\forall n \in \{0, 1, 2...\}$. ■

Theorem 4. *For $q_{non} \in \mathcal{Q}_{FES_{non}}$, the error system defined in (18) and (19) is exponentially stable, provided some gain conditions are satisfied.*

Proof: When $q_{non} \in Q_{FES_{non}}$, $\sigma_{s_{non}} = 1$ and $\sigma_{e_{non}} = 0$. Therefore, the expression in (34) can be reduced to

$$\begin{aligned} \dot{V}_{L_2} \quad = \quad & -rB_{M_{non}} \left(k_5 r + sgn\left(r\right) \left[k_6 + k_7 \left\| z \right\| \right. \right. \\ & \left. \left. + k_8 \left\| z \right\|^2 \right] \right) + r\chi_{non} - \alpha e_2^2. \end{aligned} \tag{37}$$

Upper bounding (37) using (21) and Property 8, and rearranging, yields

$$\begin{aligned} \dot{V}_{L_2} \quad \leq \quad & -c_{b_M} k_5 r^2 - \alpha e_2^2 - \left(c_{b_M} k_6 - c_3 \right) |r| \\ & - \left(c_{b_M} k_7 - c_4 \right) |r| \ \|z\| - \left(c_{b_M} k_8 - c_5 \right) |r| \ \|z\|^2, \end{aligned} \tag{38}$$

which is negative definite provided gain conditions are satisfied. Algebraic manipulation can be used to yield exponential convergence $\forall t \in \left[t^s_{n,\, non},\, t^e_{n+1,\, non} \right)$, $\forall n \in \{0, 1, 2...\}$. ■

Remark 2. By Theorems 3 and 4, and since V_{L2} is a common Lyapunov function for switching between FES and the motor on the non-dominant side, exponential convergence of the non-dominant subsystem is guaranted $\forall q_{non} \in Q$.

V. Experiments

Experiments were conducted to evaluate the performance of the FES and motor controllers developed for the dominant (given in (15) and (16)) and the non-dominant (given in (22) and (23)) subsystems. Experiments were performed on an able-bodied 24 year old female, who gave written consent approved by the University of Florida Institutional Review Board. The participant was instructed to provide no volitional contribution to the pedaling effort.

A. Split-Crank Motorized FES-Cycling Testbed

A commercially available recumbent tricycle (Terra Trike Rover X8) was modified for stationary FES-cycling, as in [4], but with the cycle crank split into decoupled right and left pedals such that there was no mechanical engagement between each side. Two of the following, one for each side, were necessary: 250 W 24V DC motors, ADVANCED Motion Controls (AMC)[3] PS300W24 power supplies, AMC AB25A100 motor drivers, and optical encoders (US Digital H1).

A current-controlled stimulator (Hasomed RehaStim) delivered biphasic, symmetric, and rectangular pulses to the participant's muscle groups via self-adhesive electrodes[4]. The stimulation amplitude was fixed at 90mA, 80mA, and 70mA for the quadriceps, gluteals, and hamstrings, respectively. The stimulation intensity was controlled by pulsewidth modulation. A Quanser QPIDe data acquisition device collected signal data from the encoders and delivered motor current. The FES and motor controllers were implemented on a computer running real time control software (QUARC, MATLAB/Simulink, Windows 10) at a sampling rate of 500 Hz.

B. Experimental Procedure

Electrodes were placed over the participant's muscle groups and the participant was seated on the cycle with her legs secured to the pedals with orthotic boots. The seat was adjusted to prevent hyperextension of the knee. The lengths of the lower limbs, as well as the distances between the crank and the hips, were measured and used to calculate the effective torque transfer ratios which determine the muscle and motor switching signals.

During the first 20 seconds, no FES was applied, and the motors alone were used to bring both legs to the desired cadence of 60 RPM with a constant phase difference of 180 degrees. After 20 seconds, the muscle stimulation was applied according to the switching signals and controllers described in (10), (15), and (22), respectively. For the dominant subsystem, the desired cadence $\dot{q}_{dom_d}$ remained at 60 RPM and the desired position and cadence for the non-dominant leg, q_{non_d} and $\dot{q}_{non_d}$, were defined as $q_{non_d} \triangleq q_{dom} - \pi$ and $\dot{q}_{non_d} \triangleq \dot{q}_{dom}$.

[3]ADVANCED Motion Controls supported the development of this testbed by providing discounts on their branded items.

[4]Surface electrodes for this study were provided compliments of Axelgaard Manufacturing Co., Ltd.

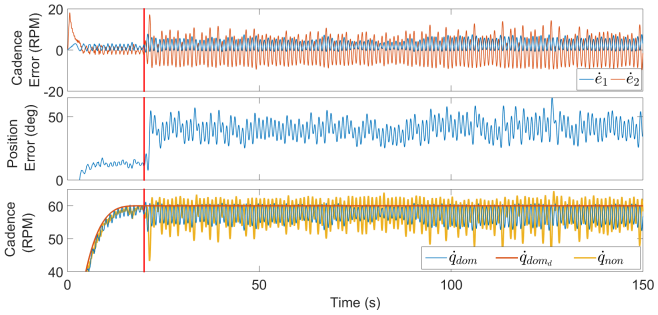

Figure 1. Tracking performance for the dominant (right) side and non-dominant (left) side including cadence error (top) for the dominant (blue) and non-dominant (orange) sides; position error e_2 for the non-dominant side (middle); and cadence (bottom) for the dominant (blue) and non-dominant (yellow) sides, in comparison to the desired cadence $\dot{q}_{dom_d}$ (orange). For illustrative purposes, the data was filtered with a 0.5s moving average. The vertical red lines at 20 seconds denote when steady state was reached.

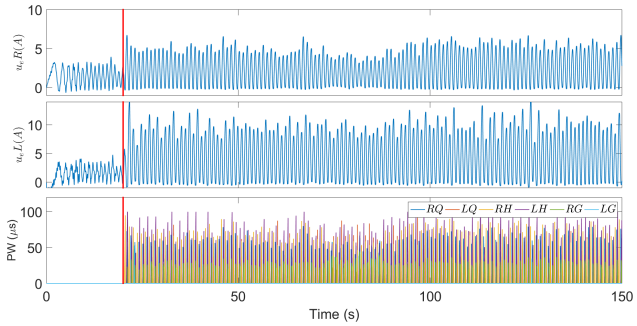

Figure 2. Motor input for the right side (top) and left side (middle), and the FES control input to both the right and left limbs (bottom). For illustrative purposes, the data was filtered with a 0.5s moving average. The vertical lines at 20 seconds denote when steady state was reached.

C. Results

The tracking performance of the 150 second trial is depicted in Figure 1 for both the dominant and non-dominant subsystems, and can also be quantified by errors e_1, $\dot{e}_1$, e_2, and $\dot{e}_2$. The average cadence and positions errors, calculated after the motor brought the legs up to speed, were 2.62 ± 3.54 RPM for the right side, and -0.04 ± 8.79 RPM and 39.84 ± 10.77 degrees for the left side. Note that in the bottom plot of Figure 1, the right side (blue) is tracking the desired cadence (red), but the left side is tracking the fluctuating real-time cadence of the right side. Figure 2 depicts the motor and FES control inputs for both sides over the duration of the trial.

D. Discussion

Figures 1 and 2 demonstrate the performance of the FES controllers in (15) and (22) and the motor current controllers

in (16) and (23). Stable tracking of cadence (for the dominant leg) and position and cadence (for the non-dominant leg) is achieved. Since the left side was tracking the measured position and cadence of the right side (as opposed to tracking a constant cadence value, as was the right side), performance was much more volatile and resulted in a higher error and standard deviation. Moreover, the right and left cadence differential (i.e., $\dot{e}_2$) was centered near zero so the pedals never became completely out of phase (i.e., the left side never "caught up" to the right side). With the larger error, the average current supplied to the left motor was nearly twice as much as the current supplied to the right (see Figure 2).

On a standard cycle with coupled pedals, mechanical engagement at the crank axis provides counterbalancing torques from one side to the other, in particular gravitational torques. On the split-crank cycle, however, the gravitational torques are not balanced, and each leg accelerates when moving down and decelerates when moving up, yielding an innate cyclical cadence fluctuation resulting in standard deviations larger than other previous FES-cycling studies [4]. The region of the crank cycle for efficient hamstring torque production coincides with the upward motion of the leg/gravity compensation, so the hamstrings generally received the highest amount of stimulation, as shown in Figure 2. The quadriceps and gluteals, however, received smaller amounts of stimulation since their effective torque regions coincided with gravity acting as an assistive torque.

VI. Conclusion

The FES-cycling controllers developed in this paper were designed to enable a rider to pedal at a desired cadence while maintaining a constant crank angle difference of 180 degrees when pedaling on a split-crank stationary cycle. A Lyapunov-like stability analysis was used to prove the stability of the controllers for the dominant and non-dominant subsystems, along with exponential tracking for the error signals. An experiment performed on an able-bodied individual validated the controllers' performance at 60 RPM.

The developed control system for a split-crank cycle has the potential to advance motorized FES rehabilitation for people with asymmetric movement disorders. Decoupled dynamics for the leg subsystems allows for each leg to contribute proportional to their abilities, preventing a person from relying on their stronger leg.

Future experiments will be performed on individuals with asymmetric NDs and could investigate adaptive methods to account for system dynamics.

References

[1] J. S. Petrofsky, H. Heaton, and C. A. Phillips, "Outdoor bicycle for exercise in paraplegics and quadriplegics," *J. Biomed. Eng.*, vol. 5, pp. 292–296, Oct. 1983.

[2] D. J. Pons, C. L. Vaughan, and G. G. Jaros, "Cycling device powered by the electrically stimulated muscles of paraplegics," *Med. Biol. Eng. Comput.*, vol. 27, no. 1, pp. 1–7, 1989.

[3] J. S. Petrofsky and J. Smith, "Three-wheel cycle ergometer for use by men and women with paralysis," *Med. Biol. Eng. Comput.*, vol. 30, pp. 364–369, 1992.

[4] M. J. Bellman, R. J. Downey, A. Parikh, and W. E. Dixon, "Automatic control of cycling induced by functional electrical stimulation with electric motor assistance," *IEEE Trans. Autom. Science Eng.*, vol. 14, no. 2, pp. 1225–1234, April 2017.

[5] D. Liberzon, *Switching in Systems and Control*. Birkhauser, 2003.

[6] H. Yang, B. Jiang, and V. Cocquempot, "A survey of results and perspectives on stabilization of switched nonlinear systems with unstable modes," *Nonlin. Anal.: Hybrid Syst.*, vol. 13, pp. 45–60, Aug. 2014.

[7] C. Rouse, C. Cousin, V. H. Duenas, and W. E. Dixon, "Cadence tracking for switched FES cycling combined with voluntary pedaling and motor resistance," in *Proc. Am. Control Conf.*, 2018, pp. 4558–4563.

[8] M. J. Bellman, T. H. Cheng, R. J. Downey, C. J. Hass, and W. E. Dixon, "Switched control of cadence during stationary cycling induced by functional electrical stimulation," *IEEE Trans. Neural Syst. Rehabil. Eng.*, vol. 24, no. 12, pp. 1373–1383, 2016.

[9] C. Cousin, V. H. Duenas, C. Rouse, and W. E. Dixon, "Stable cadence tracking of admitting functional electrical stimulation cycle," in *Proc. ASME Dyn. Syst. Control Conf.*, 2018.

[10] V. H. Duenas, C. A. Cousin, A. Parikh, P. Freeborn, E. J. Fox, and W. E. Dixon, "Motorized and functional electrical stimulation induced cycling via switched repetitive learning control," *IEEE Trans. Control Syst. Tech.*, to appear, DOI: 10.1109/TCST.2018.2827334.

[11] C. A. Cousin, C. A. Rouse, V. H. Duenas, and W. E. Dixon, "Position and torque control via rehabilitation robot and functional electrical stimulation," in *IEEE Int. Conf. Rehabil. Robot.*, 2017.

[12] V. Duenas, C. A. Cousin, C. Rouse, and W. E. Dixon, "Extremum seeking control for power tracking via functional electrical stimulation," in *Proc. IFAC Conf. Cyber. Phys. Hum. Syst.*, 2018, pp. 164–169.

[13] S. P. Hooker, S. F. Figoni, M. M. Rodgers, R. M. Glaser, T. Mathews, A. G. Suryaprasad, and S. C. Gupta, "Physiologic effects of electrical stimulation leg cycle exercise training in spinal cord injured persons," *Arch. Phys. Med. Rehabil.*, vol. 73, no. 5, pp. 470–476, 1992.

[14] T. Johnston, B. Smith, O. Oladeji, R. Betz, and R. Lauer, "Outcomes of a home cycling program using functional electrical stimulation or passive motion for children with spinal cord injury: a case series," *J. Spinal Cord Med.*, vol. 31, no. 2, pp. 215–21, 2008.

[15] S. Ferrante, A. Pedrocchi, G. Ferrigno, and F. Molteni, "Cycling induced by functional electrical stimulation improves the muscular strength and the motor control of individuals with post-acute stroke," *Eur. J. Phys. Rehabil. Med.*, vol. 44, no. 2, pp. 159–167, 2008.

[16] T. Mohr, J. Pødenphant, F. Biering-Sørensen, H. Galbo, G. Thamsborg, and M. Kjær, "Increased bone mineral density after prolonged electrically induced cycle training of paralyzed limbs in spinal cord injured man," *Calcif. Tissue Int.*, vol. 61, no. 1, pp. 22–25, 1997.

[17] C. L. Sadowsky, E. R. Hammond, A. B. Strohl, P. K. Commean, S. A. Eby, D. L. Damiano, J. R. Wingert, K. T. Bae, and I. John W. McDonald, "Lower extremity functional electrical stimulation cycling promotes physical and functional recovery in chronic spinal cord injury," *J. Spinal Cord Med.*, vol. 36, no. 6, pp. 623–631, 2013.

[18] D. Kuhn, V. Leichtfried, and W. Schobersberger, "Four weeks of functional electrical stimulated cycling after spinal cord injury: a clinical study," *Int. J. Rehab. Res.*, vol. 37, pp. 243–250, March 2014.

[19] H. Chen, S. Chen, J. Chen, L. Fu, and Y. Wang, "Kinesiological and kinematical analysis for stroke subjects with asasymmetric cycling movement patterns," *J. Electromyogr. Kinesiol.*, vol. 15, no. 6, pp. 587–595, Dec 2005.

[20] E. Ambrosini, S. Ferrante, T. Schauer, G. Ferrigno, F. Molteni, and A. Pedrocchi, "Design of a symmetry controller for cycling induced by electrical stimulation: preliminary results on post-acute stroke patients," *Artif. Organs*, vol. 34, no. 8, pp. 663–667, Aug. 2010.

[21] M. Van der Loos, L. Worthen-Chaudhari, and D. Schwandt, "A split-crank bicycle ergometer uses servomotors to provide programmable pedal forces for studies in human biomechanics," *IEEE Trans. Neural Syst. Rehabil. Eng.*, vol. 18, no. 4, pp. 445–52, April 2010.

[22] L. Ting, S. Kautz, D. Brown, and F. Zajac, "Contralateral movement and extensor force generation alter flexion phase muscle coordination in pedaling," *J. Neurophysiol.*, vol. 83, no. 6, pp. 3351–65, Jun 2000.

[23] E. S. Idsø, T. Johansen, and K. J. Hunt, "Finding the metabolically optimal stimulation pattern for FES-cycling," in *Proc. Conf. of the Int. Funct. Electrical Stimulation Soc.*, Bournemouth, UK, Sep. 2004.

[24] M. J. Bellman, T.-H. Cheng, R. J. Downey, and W. E. Dixon, "Stationary cycling induced by switched functional electrical stimulation control," in *Proc. Am. Control Conf.*, 2014, pp. 4802–4809.